Solvable splines for direct and inverse modeling of media with graded properties

Jean-Claude KRAPEZ

ONERA, The French Aerospace Lab, 13661 Salon de Provence, France

krapez@onera.fr

Graded media, i.e. media with continuous variation in their properties, are ubiquitous. Examples can be found at different scales in nature (soils, wood, living tissues: e.g. skin, teeth, boundary layers in the atmosphere and the ocean) and in manmade materials (functionally graded materials -FGM- as for examples composites, thermal barriers, optical thin films, Bragg gratings, tapered transmission lines and many others). In 1D graded media, thermal diffusion is driven by the effusivity profile. On the other side, electromagnetic (EM) wave propagation is driven by the EM admittance profile (or simply the refractive index, in non-magnetic materials). A method has recently been described for the construction of sequences of effusivity profiles that are "solvable", which means profiles leading to exact analytical solutions for the time- (or frequency-) dependent temperature [1]. The proposed profiles are expressed in closed-form, involving elementary functions only (the same holds for the corresponding temperature solution when expressed in the Fourier or Laplace space). Similar sequences have been proposed in the context of Maxwell's equations for lossless media, more generally for a class of wave equations to which acoustic waves and electric waves in LC transmission lines also belong, just to name a few [2]. In all these cases, the solvable profiles together with their joint field-solutions are generated by applying repeatedly the Darboux transformation in the Liouville space (PROFIDT method: PROperty and FIeld Darboux Transformation method). At each iteration, the number of leading parameters increases, which improves the fitting capability of the profiles. In the Liouville space, depending on the considered problem, i.e. thermal diffusion or (optical/acoustical) wave scattering, the new independent-variable ξ corresponds to the (square-root of) diffusion-time (SRDT), resp. the optical-depth (or acoustical-depth). In the Liouville space, the solvable profiles share the same form, for both considered problems (diffusion or wave scattering). One class of solvable profiles is particularly interesting, we dubbed it "profiles of $\mathrm{sech}\left(\hat{\xi}\right)$-type" because they are defined through a linear combination of two independent functions, the first one being the hyperbolic secant function ($\mathrm{sech} = 1/\cosh$) of the linearly deformed ξ-variable, namely $\hat{\xi} = \xi/\xi_c + \tau$. In the thermal context, the $\mathrm{sech}\left(\hat{\xi}\right)$-type profiles of effusivity are defined by:

$$b^{\pm 1/2}(\xi) = A_B B(\xi) + A_D D(\xi) \quad ; \quad \begin{cases} B(\xi) = \mathrm{sech}\left(\hat{\xi}\right) \\ D(\xi) = \sinh\left(\hat{\xi}\right) + \hat{\xi}\,\mathrm{sech}\left(\hat{\xi}\right) \end{cases}$$

The "$+1/2$" exponent refers to profiles called of $\langle T \rangle$-form and the "$-1/2$"exponent refers to profiles called of $\langle \varphi \rangle$-form (as a matter of fact, they originate from the heat equation expressed in temperature, resp. in heat flux).

In addition to the outstanding properties already mentioned, these four-parameter profiles are extremely flexible. This means that we can adjust the four parameters ξ_c, τ, A_B and A_D so that the considered property (either thermal effusivity, EM admittance or refractive index) and its slope at both boundaries of a given layer reach any given set of four values. Hence, composite profiles of arbitrary shape can be built by assembling such elementary bricks [3, 4]. The corresponding (exact) field-solution (temperature or electric field) is then obtained based on transfer-matrix multiplications like in the classical quadrupole method. As opposed to the classical quadrupole method where each layer is assumed to be homogeneous, the individual layers now present continuously variable properties. The whole functional may be continuous at the nodes up to the second derivative. Hence, it can be manipulated like an interpolating spline function. It is the first known class of "solvable splines" aimed at modeling both diffusion and wave-like problems in graded media.

The next figure intends to illustrate the case of a graded coating in which, starting from the surface, the effusivity first decreases to a minimum and then increases to the bulk value. In this figure, the effusivity is normalized by the bulk value and the depth is represented through the SRDT which has been normalized by the value ξ_{end} corresponding to the depth where effusivity reaches the bulk value. Three curves have been plotted. The blue curve is the classical cubic spline as obtained after specifying the position and height of three nodes together with the slope at both ends of the coating (this corresponds to a "clamped spline"; in this example, the normalized slope is set to -2 at left-end and 0 at right-end). On each of two intervals, two $\mathrm{sech}\left(\hat{\xi}\right)$-type profiles have been evaluated, one of $\langle T \rangle$-form (in black) and one of $\langle \varphi \rangle$-form (in red). The value and derivative of the cubic spline at both ends of each interval provide the four constraints used to evaluate the four parameters of each $\mathrm{sech}\left(\hat{\xi}\right)$-type profile. For the effusivity values and derivatives considered in this example, the $\langle T \rangle$-form and $\langle \varphi \rangle$-form profiles are very close one to the other. Furthermore, they are not very different from each element of the cubic-spline. Then, a composite profile is obtained by stitching two successive $\mathrm{sech}\left(\hat{\xi}\right)$-type profiles. Notice that profiles of $\langle T \rangle$-form and $\langle \varphi \rangle$-form can be freely mixed, which, in the example described here, gives four (slightly) different composite profiles. Remember that each composite profile is a *solvable profile* in the sense that temperature and heat flux at each position can be analytically calculated by combining in due order the quadrupoles related to each elementary profiles. This is not the case with the cubic-spline profile for which there is no closed-form analytic solution.

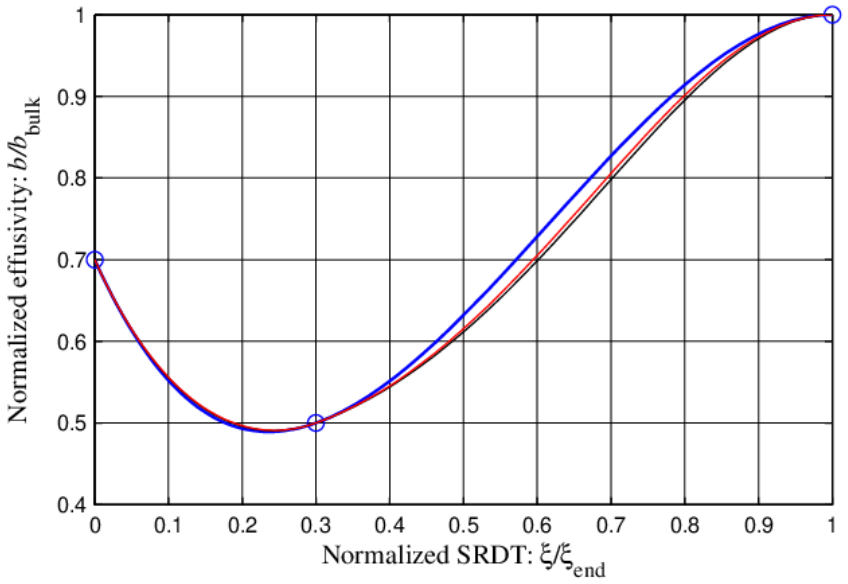


Fig. 1. Comparison between the classical cubic spline (in blue) and the *solvable splines* of $\mathrm{sech}\left(\hat{\xi}\right)$-type of either $\langle T \rangle$-form (in black) or $\langle \varphi \rangle$-form (in red).

The inversion problem consists in finding the *composite solvable profile* whose temperature solution best matches with the experimental temperature data measured on the surface of the functionally graded material. One possible strategy is to select a small number of nodes and perform the fitting by adjusting the ξ-position of the internal nodes, together with the effusivity and slope at each node. Different avenues can be explored regarding the constraint on the left vs. right values of effusivity or its derivative at each node (i.e. continuous vs. discontinuous profile or broken vs. smooth profile).

The differential equations to which the proposed PROFIDT method can be applied are quite general, which means that the proposed tools can be implemented to find exact analytical solutions in graded media for a whole bunch of problems in addition to those already quoted: matter diffusion (Fick's law), Stokes problems, advection-diffusion, microfluidic, tapered RC or LC transmission lines, longitudinal acoustic waves, shear waves, ocean gravity waves, etc.

Several examples of applications will be presented related to thermal problems (photothermal characterization), to advection-diffusion problems (pollutant dispersion in the atmosphere, footprint modeling for soil-atmosphere flux studies) and to photonic problems (rugate filters, chirped mirrors, antireflection layers).

References

1. J.-C. Krapez, Int. J. Heat Mass Transfer, **99**, 485-503 (2016) https://doi.org/10.1016/j.ijheatmasstransfer.2016.03.122
2. J.-C. Krapez, J. Modern Optics, **64**(19), 1988-2016 (2017) https://doi.org/10.1080/09500340.2017.1330975
3. J.-C. Krapez, Int. J. Thermophysics, **39**(7), 86 (2018), https://doi.org/10.1007/s10765-018-2406-z
4. J.-C. Krapez, J. Opt. Soc. Am. A, **35**(6), 1039-1052 (2018), https://doi.org/10.1364/JOSAA.35.001039